Available online at www.sciencedirect.com
ScienceDirect
Computational Materials Science 43 (2008) 715–723
COMPUTATIONAL MATERIALS SCIENCE
www.elsevier.com/locate/commatsci

Continuum structures equivalent in normal mode vibrations to single-walled carbon nanotubes

S.S. Gupta, R.C. Batra *

Department of Engineering Science and Mechanics, M/C 0219, Virginia Polytechnic Institute and State University, Blacksburg, VA 24061, USA

Received 14 December 2007; received in revised form 7 January 2008; accepted 16 January 2008
Available online 7 March 2008

Abstract

Axial, torsional and radial breathing mode (RBM) vibrations of free–free unstressed (i.e., relaxed) single-walled carbon nanotubes (SWCNTs) of different helicities having aspect ratio (length/diameter) of about 15 have been studied using the MM3 potential. It is found that for axial and torsional vibrations, frequencies of the second and the third modes of SWCNTs equal, respectively, twice and three times that of the corresponding first mode. A similar relation also holds for axial and torsional vibrations of a homogeneous linear elastic prismatic body. The RBM frequencies are also used to validate computed frequencies of SWCNTs.

Equivalent continuum structures (ECSs) whose frequencies in axial, torsional and radial breathing modes are equal to those of the SWCNTs are identified. The consideration of free ends eliminates the effect of boundary conditions and avoids resolving equivalence between boundary conditions in the analysis of SWCNTs and their ECSs. It is found that the ECS made of a linear elastic homogeneous material is a cylindrical tube of mean radius and length equal to those of the SWCNT. Poisson's ratio of the ECS (and hence of the SWCNT) computed without assuming any value for the wall thickness converges with an increase in the diameter of the SWCNT to 0.20 for armchair, 0.23 for zigzag, and 0.21 for chiral tubes. For a wall thickness of the ECS equal to 3.4 Å, Young's modulus of the material of the ECS (and hence of the SWCNT) equals ~1 TPa and is independent of the helicity and the diameter of the SWCNT. However, the shear modulus varies with the diameter and the helicity of the underlying SWCNT. In the more common terminology, normal modes of vibrations of a SWCNT give Young's modulus of ~1 TPa in the axial and the circumferential directions, and the shear modulus of ~0.4 TPa. Whereas Young's modulus of a SWCNT is found to be independent of its diameter and helicity, the shear modulus depends weakly upon them.

PACS: 46.70.Lk

Keywords: Elastic moduli; Equivalent continuum structures; Vibrations

1. Introduction

Since their discovery by Iijima [1] in 1991, there has been significant interest in characterizing mechanical properties of both single-walled carbon nanotubes (SWCNTs) and multi-walled carbon nanotubes (MWCNTs). An inherent difficulty in completing this task is assigning a thickness to the nanotube. Nearly all studies to date have assumed that the response of a SWCNT is equivalent to that of a continuum structure undergoing deformations similar to those of the SWCNT. The ECS (equivalent continuum structure) could either be a solid fiber or a cylindrical tube. However, in order that an ECS account at least approximately for the effect of van der Waals forces prevalent in a CNT, we assume that the ECS of a SWCNT is a cylindrical tube and that of a MWCNT is comprised of co-axial cylindrical tubes of lengths and mean radii equal to those of the corresponding CNTs [2]. The remaining variables of the ECS to be found are the thickness, and values of material moduli, and the mass density.

* Corresponding author. Tel.: +1 540 231 6051; fax: +1 540 231 4574.
E-mail address: rbatra@vt.edu (R.C. Batra).

0927-0256/$ - see front matter © 2008 Elsevier B.V. All rights reserved.
doi:10.1016/j.commatsci.2008.01.032

The determination of the ECS is important since it facilitates computing with either a homogenization technique or a micromechanical analysis effective moduli and mass density of a composite with CNTs as reinforcements, which are needed in the design of structures. Furthermore, it is crucial to know whether or not the same ECS ought to be used when studying static and dynamic deformations of a SWCNT reinforced composite.

To simplify the work one assumes that the ECS is made of a homogeneous material. What about the symmetry group of the material of the ECS? Said differently, should the material of the ECS be taken as isotropic or anisotropic? If it is anisotropic, is it transversely isotropic or orthotropic or has some other material symmetry group? We note that expressions for molecular mechanics (MM) potentials involve distances between atoms and angles between lines joining adjacent atoms. These distances and angles are invariant under a full orthogonal group. Thus a rigid translation and a rotation of a SWCNT will not alter the value of the MM potential. However, one expects intuitively that material properties of the ECS in the radial direction should be different from those in the axial and the circumferential direction since a SWCNT is only one atom thick. Also, contributions to the MM potential from bonded and non-bonded atoms during radial deformations will be different from those when the tube is deformed axially. Thus the symmetry group of an ECS is determined by the relative positions of atoms in the corresponding CNT as in body-centered cubic and face-centered cubic crystals.

It is commonly assumed that a SWCNT is obtained by rolling a graphene sheet into a cylindrical tube. We adopt this assumption and further postulate that the response of a graphene sheet is the same in all directions in its plane but may be different from that in the thickness direction. We thus regard the material of the ECS to be transversely isotropic with the axis of transverse isotropy along the radial direction, similar to that presumed by Batra and Sears [3]. It implies that Young's moduli in the axial and the circumferential directions are same but may be different from that in the radial direction.

Whereas a molecular mechanics/dynamics (MM/MD) potential used to characterize the response of a SWCNT allows for long range interactions between atoms, the ECS is generally assumed to be made of either linear elastic or a non-linear elastic material with response depending upon local interactions among material points. It reduces the number of unknowns to be determined in order to characterize the ECS material. For infinitesimal deformations from the unstressed or the natural or the relaxed state of a SWCNT and of the ECS, it is reasonable to regard their responses to be linear elastic. Hence we need to find values of five material moduli of the transversely isotropic material of the ECS which in common terminology are called the elastic moduli of the SWCNT.

One invariably assumes that the ECS is deformed homogeneously, and the ECS and the SWCNT have the same overall strains. This analogy works well for simple deformations such as axial tension/compression. For torsional, bending and radial expansion/contraction of SWCNTs and their ECSs, it is a non-trivial task to find an equivalence between deformations of the two structures since a SWCNT is an atom thick and the ECS has a finite thickness. Unless the thickness/(mean radius) of the ECS is much smaller than one, its bending and torsional deformations will vary noticeably through the thickness.

A continuum structure can generally be deformed homogeneously only if ideal boundary conditions are prescribed at the bounding surfaces. Near the end faces where either displacements or surface tractions are assigned, deformations are usually inhomogeneous. Only at material points far away (usually about two diameters) from the boundary points, deformations are homogenous or nearly homogeneous. This requires establishing a proper equivalence between boundary conditions assigned at end faces of a CNT and those of its ECS.

Sears and Batra [4] have listed in Tables 1 and 2 of their paper values of the thickness of the ECS used by various investigators to find the axial modulus of either a SWCNT or a MWCNT. The non-uniqueness in the thickness of the ECS results in different values of material moduli of the ECS and hence of the CNT. Sears and Batra [4] proposed that the thickness be found by using the relation $E = 2G(1 + \nu)$ between the axial Young's modulus E, the shear modulus G, and Poisson's ratio ν – all three measured in the plane of the graphene sheet. For the response of the $(16, 0)$ SWCNT modeled by the MM3 potential, they first determined $\nu = 0.21$ by finding the change in the diameter of the SWCNT when it is pulled axially, and then used the relation between E, G and ν to get $E = 7.26$ TPa, $G = 3$ TPa, and wall thickness $h = 0.4593$ Å.

The wall thickness so found is different from the 0.66 Å and the 3.4 Å employed by several investigators. Of course, values of E and G depend upon the wall thickness and the MM potential employed. Results of several other investigations [5–22] not listed by Sears and Batra [4] are summarized below in Table 1. We note that the wall thicknesses used vary from 1.29 Å to 6.8 Å. These investigators may have used CNTs of different helicities and diameters besides employing different techniques and MM potentials to simulate their deformations. The axial Young's modulus computed by these researchers varies between 0.69 and 1.36 TPa, Poisson's ratio between 0.14 and 0.43, and the shear modulus between 0.14 and 0.65 TPa. They assumed the ECS material to be homogeneous, linear elastic and isotropic.

Here we study vibrations of free–free SWCNTs of different diameters and helicities with aspect ratio of about 15, and compare their frequencies with those of their ECSs. The consideration of free ends eliminates establishing equivalence between boundary conditions for CNTs and their ECSs. We briefly review some works on vibrations of CNTs. Sohlberg et al. [23] employed the solution of wave equation, and simple beam dynamics to relate vibrations of a CNT in terms of those of its ECS. However,

Table 1
Values of E, G and v reported in the literature; presently computed values of these variables are listed in the last row

Researchers	Procedure	Elastic constants and thicknesses			
		E (TPa)	G (TPa)	v	h (Å)
Sanchez-Portal et al. (Ref. [6])	Ab initio	≈1.0	–	–	3.4
Goze et al. (Ref. [7])	Tight binding	1.24		0.247–0.275	3.4
Zhou et al. (Ref. [8])	First-principles	0.764	–	0.32	–
Reich et al. (Ref. [9])	First-principles	1.075	0.65	–	–
Reich et al. (Ref. [9])	Continuum	1.0	–	0.14	3.1
Jin and Yuan (Ref. [10])	MD-Energy approach	$E_\theta, E_z \approx 1.238$	$G_{\theta z} \approx 0.547$	$v_{\theta z} \approx 0.259$, $v_{z\theta} \approx 0.259$	3.4
Jin and Yuan (Ref. [10])	MD-Force approach	$E_\theta, E_z \approx 1.350$	$G_{\theta z} \approx 0.492$		
Li and Chou (Ref. [11])	Structural mechanics	≈1.04	≈0.48	–	3.4
Natsuki et al. (Ref. [12])	Structural mechanics	≈0.61–0.48	≈0.30–0.27	0.27	3.4
Zhang et al. (Ref. [13])	Cauchy–Born rule	1.08–0.5	0.61	–	3.35
Guo et al. (Ref. [14])	Cauchy–Born rule	0.69	–	0.4295	3.34
Huang et al. (Ref. [15])	Interatomic Potential	0.55–1.23	–	–	3.41
Kalamkarov et al. (Ref. [16])	Analytical-asymptotic homogenization model	1.44	0.27	–	1.29
Kalamkarov et al. (Ref. [16])	Finite element	0.97–1.05	0.14–0.47	–	6.8
Wu et al. (Ref. [17])	MM–continuum	1.06	0.418	0.273	2.58
Peng et al. (Ref. [18])	Ab initio	1.23–1.36	–	–	3.4
To (Ref. [19])	Finite element	1.024	0.47	–	3.4
Chandraseker and Mukherjee (Ref. [20])	Atomistic–continuum	≈0.46–0.68	≈0.186–0.236	–	3.35
Chandraseker and Mukherjee (Ref. [20])	Ab initio	0.906–0.990	–	–	3.35
Poncharal et al. (Ref. [21])	TEM	1.2 – 0.2	–	–	–
Agrawal et al. (Ref. [22])	MD–continuum	0.73 – 0.82	–	–	3.4
Present	MM–continuum	0.964 ± 0.035	0.403 ± 0.025	0.14–0.249	3.4

while studying the radial breathing mode (RBM) vibrations of a CNT and of its ECS, they seem to have ignored the fact that radial deformations of a tube wall induce strains in both the radial and the circumferential directions. Yao and Lordi [24] analyzed transverse and longitudinal thermal oscillations of a cantilever CNT using MD potential based on a universal force field. For a wall thickness of 3.4 Å, they found that the axial Young's modulus of the ECS decreased with an increase in the SWCNT diameter and eventually approached 0.98 TPa. It is likely that for tubes of large diameters studied by Yao and Lordi [24] the tube lengths were not large enough for the expression for the frequency of transverse vibration to be applicable. Krishnan et al. [25] experimentally studied thermally induced stochastic vibrations of cantilever SWCNTs with diameters in the range of 10–15 Å, and found the average value of Young's modulus to be 1.25 TPa. Poncharal et al. [21] assumed that the ECS is a solid fiber, used Euler's beam theory to analyze its vibrations, and found that for SWCNTs of diameters 8 and 30 nm, Young's modulus equaled 1.2 and 0.2 TPa respectively. Because of rather large diameters of CNTs, the tubes may not have been long enough for the Euler beam theory to be applicable. Agrawal et al. [22] used MD simulations to analyze transient axial and transverse deformations of a cantilever SWCNT, and found Young's modulus at either a constant value of the axial stress or a constant value of the axial strain. The average value of Young's modulus for armchair and zigzag SWCNTs was found to be 0.73 and 0.82 TPa, respectively.

Wang et al. [26] have studied the applicability of Donnell's and Flugge's shell theories to ECSs for SWCNTs. They found that predictions for the latter theory correlate well with deformations of SWCNTs computed from MM/MD simulations.

The rest of the paper is organized as follows. Section 2 describes the MM3 potential, and Section 3 provides details of our MD simulations of the axial, the torsional, and the RBM vibrations of free–free SWCNTs with no cut-off distance used. Results of MD simulations are given in Section 4. Section 5 briefly reviews known results of axial, torsional and RBM vibrations of a cylindrical tube made of a homogeneous linear elastic material. In Section 6 we compare results of MD simulations with those of linear elasticity, assume the wall thickness of the ECS to be 3.4 Å, and derive values of the axial Young's modulus, the shear modulus and Poisson's ratio of the material of the ECS, and hence of the SWCNT.

It is shown in Section 7 that these values agree well with those computed from MM3 simulations of static axial and torsional deformations of SWCNTs, and are also close to those found by other investigators.

2. Molecular dynamics potential

The MM3 class II pair-wise potential with both higher-order expansions and cross-terms and type 2 (alkene) carbon atoms [27] with a bond length of 1.42 Å is used. This potential is appropriate for CNTs due to the similarity between graphitic bonds in the nanotube and the aromatic protein structures for which the potential was constructed.

The MM3 potential is given as Eq. (1) in which U_s, U_θ and U_ϕ are the primary bond deformation terms; U_{vdW} is the potential of non-bonded van der Waals forces, and

Table 2
Geometry, number of atoms and frequencies of first three modes of torsional and axial vibrations of relaxed SWCNTs and values of Poisson's ratio, and Young's and shear moduli of ECSs

Tube	Geometry/ Atoms (r_o, l_o) Å (r_e, l_e) Å n_c	Mode	Torsional (cm^{-1})	Axial (cm^{-1})	v	E (TPa)	G (TPa)
(5,0)	(1.957, 59.640)	1	37.546	58.006	0.193	0.936	0.392
	(1.869, 55.425)	2	74.994	115.842	0.193	0.934	0.391
	280	3	112.243	173.311	0.192	0.929	0.390
(5,5)	(3.390, 103.299)	1	22.270	33.730	0.147	0.985	0.429
	(3.222, 97.043)	2	44.541	67.384	0.144	0.983	0.429
	840	3	66.818	100.878	0.140	0.979	0.429
(10,0)	(3.915, 119.280)	1	18.732	29.633	0.251	0.999	0.399
	(3.716, 112.969)	2	37.464	59.218	0.249	0.998	0.399
	1120	3	56.161	88.698	0.252	0.995	0.399
(9,6)	(5.119, 167.120)	1	13.622	20.893	0.176	0.977	0.415
	(4.856, 158.100)	2	27.244	41.753	0.174	0.976	0.415
	2052	3	40.866	62.542	0.176	0.973	0.415
(8,8)	(5.425, 164.787)	1	13.833	21.161	0.170	0.971	0.415
	(5.146, 155.261)	2	27.667	42.284	0.168	0.969	0.415
	2144	3	41.503	63.321	0.164	0.966	0.415
(14,2)	(5.911, 182.253)	1	12.282	19.276	0.231	0.992	0.403
	(5.606, 172.808)	2	24.561	38.522	0.230	0.991	0.403
	2584	3	36.840	57.710	0.227	0.988	0.403
(9,9)	(6.103, 184.463)	1	12.319	18.902	0.177	0.971	0.412
	(5.787, 173.879)	2	24.637	37.769	0.175	0.969	0.412
	2700	3	36.956	56.562	0.171	0.966	0.412
(16,0)	(6.264, 191.700)	1	11.633	18.329	0.241	0.938	0.378
	(5.939, 181.303)	2	23.263	36.631	0.239	0.937	0.378
	2880	3	34.891	54.871	0.236	0.9348	0.378
(10,10)	(6.780, 204.139)	1	11.101	17.077	0.183	0.971	0.410
	(6.429, 192.503)	2	22.202	34.124	0.181	0.970	0.410
	3320	3	33.304	51.104	0.177	0.967	0.410
(15,5)	(7.058, 215.035)	1	10.443	16.270	0.214	0.983	0.405
	(6.691, 203.737)	2	20.886	32.515	0.212	0.982	0.405
	3640	3	31.328	48.701	0.208	0.979	0.405
(11,11)	(7.459, 223.816)	1	10.103	15.574	0.188	0.972	0.409
	(7.071, 211.130)	2	20.206	31.122	0.186	0.970	0.409
	4004	3	30.309	46.722	0.188	0.972	0.409
(20,0)	(7.830, 238.560)	1	9.346	14.691	0.235	0.9738	0.394
	(7.422, 222.966)	2	18.691	29.359	0.233	0.9723	0.394
	4480	3	28.034	43.977	0.230	0.9696	0.394
(19,3)	(8.090, 264.085)	1	8.464	13.258	0.227	0.987	0.402
	(7.666, 250.557)	2	16.928	26.498	0.225	0.985	0.402
	5124	3	25.390	39.697	0.222	0.983	0.402
(13,13)	(8.815, 265.627)	1	8.484	13.120	0.195	0.972	0.406
	(8.355, 250.718)	2	16.969	26.217	0.193	0.970	0.406
	5616	3	25.453	39.265	0.190	0.968	0.406
(17,9)	(8.953, 292.268)	1	7.689	11.938	0.205	0.979	0.406
	(8.485, 277.197)	2	15.379	23.858	0.203	0.978	0.406
	6276	3	23.069	35.742	0.200	0.975	0.406
(23,0)	(9.004, 272.640)	1	8.177	12.837	0.232	0.973	0.395
	(8.534, 255.246)	2	16.354	25.655	0.230	0.971	0.395
	5888	3	24.530	38.428	0.227	0.968	0.395
(15,15)	(10.171, 309.898)	1	7.255	11.244	0.200	0.973	0.405
	(9.640, 292.642)	2	14.511	22.488	0.200	0.973	0.405
	7560	3	21.768	33.654	0.195	0.968	0.405

Table 2 (*continued*)

Tube	Geometry/ Atoms (r_o, l_o) Å (r_e, l_e) Å n_c	Mode	Torsional (cm^{-1})	Axial (cm^{-1})	ν	E (TPa)	G (TPa)
(26,0)	(10.179,315.240)	1	7.073	11.092	0.230	0.973	0.395
	(9.646,295.587)	2	14.145	22.168	0.228	0.971	0.395
	7696	3	21.217	33.207	0.225	0.968	0.395
(22,7)	(10.261,334.972)	1	6.682	10.424	0.217	0.981	0.403
	(9.723,317.625)	2	13.364	20.834	0.215	0.980	0.403
	8244	3	20.045	31.211	0.212	0.977	0.403

r and l are radius and length of the SWCNTs and subscripts 'o' and 'e' refer to initial and relaxed configurations.
n_c refers to number of carbon atoms in the SWCNTs.

$U_{s\phi}$, $U_{\phi s}$ and $U_{\theta\theta}$ represent cross interactions between different types of deformations. Parameters r, θ and φ used in Eq. (1) are shown in Fig. 1. A subscript, e, on a variable signifies its value in the configuration of minimum potential energy. The total energy of a body equals the sum of the potentials of all atoms in the body (the indices i and j in Eq. (1) range over bonded atoms, and the index k over all atoms).

$$
\begin{aligned}
U &= \sum_i \sum_j (U_s + U_\theta + U_\phi + U_{s\phi} + U_{\phi s} + U'_{\theta\theta}) \\
&\quad + \sum_i \sum_k U_{vdW}, \\
U_s &= 71.94 K_s (r - r_e)^2 \\
&\quad \left[1 - 2.55(r - r_e) + \left(\frac{7}{12}\right) 2.55 (r - r_e)^2\right], \\
U_\theta &= 0.021914 K_\theta (\theta - \theta_e)^2 [1 - 0.014(\theta - \theta_e) \\
&\quad + 5.6(10)^{-5} (\theta - \theta_e)^2 - 7.0(10)^{-7} (\theta - \theta_e)^3 \\
&\quad + 9.0(10)^{-10} (\theta - \theta_e)^4], \\
U_\phi &= (V_1/2)(1 + \cos\phi) + (V_2/2)(1 - \cos 2\phi) \\
&\quad + (V_3/2)(1 + \cos 3\phi), \\
U_{s\phi} &= 2.51118 K_{s\phi} [(r - r_e) + (r' - r'_e)](\theta - \theta_e), \\
U_{\phi s} &= 11.995 (K_{\phi s}/2)(r - r_e)(1 + \cos 3\phi), \\
U_{\theta\theta'} &= -0.021914 K_{\theta\theta'} (\theta - \theta_e)(\theta' - \theta'_e), \quad \text{and} \\
U_{vdW} &= \varepsilon_e \{-2.25 (r_v/r)^6 + 1.84(10)^5 \exp[-12.0(r/r_v)]\}
\end{aligned}
\tag{1}
$$

Values of constants K_s, K_θ, V_1, V_2, V_3, ε_e, r_v, $K_{s\varphi}$,, $K_{\phi s}$ and $K_{\theta\theta}$ are given in Zhou et al. [28]. Note that the van der Waals force between two atoms varies as $(r_v/r)^6$ and $\exp(-12\, r/r_v)$. The first term is the same as that in the Lennard–Jones potential, but the second term is different.

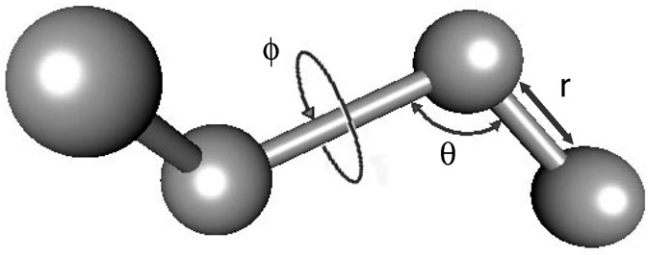

Fig. 1. Depictions of variables r, θ and ϕ used in the MM3 potential.

3. Vibrations of a SWCNT

In order to derive elastic moduli and geometric parameters of an ECS that has the same mechanical response as the corresponding SWCNT we consider SWCNTs of large aspect ratio, i.e., the length/diameter is about 15. A large aspect ratio of an ECS minimizes transverse inertia effects which are responsible for coupling among the thickness, the elastic modulus, Poisson's ratio and the frequency of axial oscillations. However, the same can not be said *a priori* for the SWCNTs since these effects have not been investigated yet. Furthermore, we do not know the effective thickness of a SWCNT since it is only one atom thick. Frequencies of the first few axial, torsional and RBMs of vibrations of a SWCNT are derived from results of MD simulations as follows.

The SWCNTs are first relaxed to find the minimum energy configuration at room temperature to within 0.001 kcal/mol/Å rms without using any cut-off distance. It is ensured that tubes in the relaxed configuration have aspect ratio of about 15. Both ends of the tube are assumed to be free to eliminate the problem of establishing equivalence between boundary conditions to be applied to SWCNTs and their ECSs. The module VIBRATE in computer code TINKER [29] is used to calculate frequencies. It computes the Hessian of the system by finding second-order derivatives of the MM3 potential with respect to positions of atoms in the relaxed configuration, and then diagonalizes the mass weighted Hessian to compute eigenvalues and eigenvectors of normal modes.

The first six eigenvalues of the Hessian equal zeros and are discarded since they correspond to three translational and three rotational rigid body modes. The eigenvector associated with an eigenvalue is used to identify the corresponding mode of vibration of a SWCNT. These are compared with the natural frequencies of the ECS for the same mode of vibration by assuming the material of the ECS to be linear elastic, homogeneous and transversely isotropic with the axis of transverse isotropy in the radial direction.

Table 3
Frequencies of radial breathing modes for SWCNTs (N.A.: not available)

Tube	Present Simulations (cm^{-1})	Present Continuum (cm^{-1})	Rao et al. [30] (cm^{-1})	Richter and Subbaswamy [31] Saito et al. [34] (cm^{-1})	Lawler et al. [35] (cm^{-1})	Kurti et al. [32] (cm^{-1})	Kuzmany et al. [33] (cm^{-1}) (Experimental)
(5,0)	568.847	556.631	N.A.	N.A.	602	N.A.	N.A.
(5,5)	332.881	333.040	N.A.	N.A.	341	N.A.	N.A.
(10,0)	290.463	294.926	N.A.	N.A.	294	298	N.A.
(9,6)	221.496	219.559	N.A.	N.A.	222	N.A.	N.A.
(8,8)	209.008	205.768	206	N.A.	210	219	211
(14,2)	192.508	194.083	N.A.	N.A.	191	N.A.	N.A.
(9,9)	185.896	183.260	183	N.A.	187	195	195
(16,0)	181.747	183.163	N.A.	N.A.	177	188 (fitted)	185
(10,10)	167.377	165.280	165	165	169	175	177
(11,11)	152.207	150.590	150	N.A.	N.A.	159	162
(20,0)	145.363	144.227	N.A.	N.A.	N.A.	150	N.A.

4. MD simulation results

Table 2 lists initial lengths and radii of various SWCNTs studied, and their lengths and radii after they have been relaxed. The diameter, d, of an (m,n) SWCNT is found from its bond length a_0 by using the relation [41]

$$d = \frac{a_0\sqrt{3}}{\pi}\sqrt{(m^2+n^2+mn)} \tag{2}$$

To check the validity of Eq. (2), the circumference of tubes in both states, the original and the relaxed, was measured and the diameter thus calculated was found to agree well with that obtained from Eq. (2). It is noted that while calculating the diameter of a relaxed tube, a_0 in Eq. (2) is set equal to the bond length in the relaxed configuration. It is clear from values listed in Table 2 that for all SWCNTs studied, the radius and the length of a relaxed tube are less than those of the starting tube. The total number of atoms used in the simulations increases with an increase in the diameter of the SWCNT. We have also listed in Table 2 frequencies of the first three torsional and the axial modes of vibration of the SWCNTs. We note that for each tube studied, the frequency of the 2nd and the 3rd mode is very close to twice and three times the corresponding frequency of the 1st mode. Frequencies in cm^{-1} equal the frequency in Hz divided by the speed of light (3×10^{10} cm/s).

Raman spectroscopy is a reliable technique to characterize SWCNTs experimentally. A peak corresponding to a RBM is a significant spectral line observed during experiments [30]. Frequencies, ω_{RBM}, of RBMs of SWCNTs are listed in Table 3, and their values are compared with those available in the literature. Since SWCNTs studied are of finite lengths, only that RBM is considered whose axisymmetric eigenvector has one half wave length along the tube axis. From results reported in Table 3, it is clear that the presently computed frequencies agree well with those found by others either computationally or experimentally. We have also plotted in Fig. 2, ω_{RBM} versus the radius of the relaxed SWCNT. The least squares fit to the data by a helicity-independent power law of the form $\omega_{\mathrm{RBM}} = B/r_{\mathrm{e}}$ (Ref. [36]) gives $B = 1076\ \mathrm{cm}^{-1}$ Å. However,

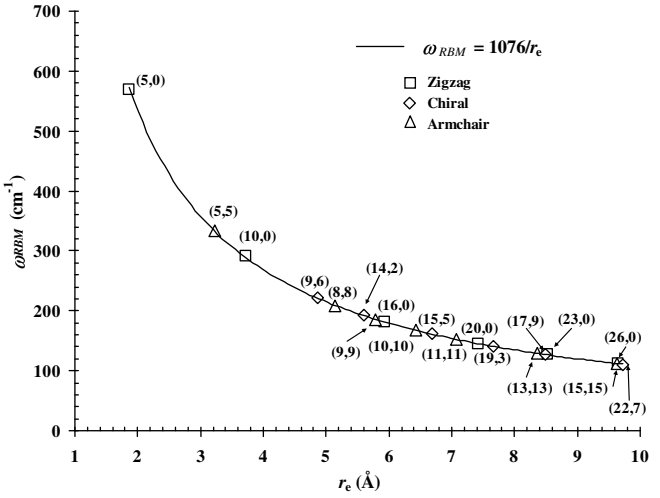

Fig. 2. Dependence of the frequency of the RBM of vibration of a SWCNT upon its radius in the relaxed configuration.

when the radius of the original (unrelaxed) SWCNT is used, then B equals $1135\ \mathrm{cm}^{-1}$ Å. Values of B in, cm^{-1} Å, reported by other investigators and based on the radius of the unrelaxed tube are 1090 [37], 1140 [38], 1160 [6], 1170 [32], 1155 [35] and 1119 [38]. Thus the presently computed value of B is in good agreement with that obtained by other researchers. However, we believe that the radius of the relaxed SWCNTs should be considered in the relation $\omega_{\mathrm{RBM}} = B/r_{\mathrm{e}}$. Thus the relation $\omega_{\mathrm{RBM}} = B/r_{\mathrm{e}}$ between the computed ω_{RBM} and r_{e} agrees with that obtained using other techniques.

5. Review of natural frequencies of a continuous structure

Natural frequencies of axial and torsional modes of vibration of a free–free cylindrical continuum rod or tube made of a linear elastic, homogeneous and transversely isotropic material with the axis of transverse isotropy along a radial line are given by [39]

$$\omega_{n\mathrm{A}} = \frac{n\pi}{l_{\mathrm{e}}}\sqrt{\frac{E}{\rho}}; \quad n = 1,2,3,\ldots; \text{ for axial oscillations} \tag{3}$$

$$\omega_{n\mathrm{T}} = \frac{n\pi}{l_e}\sqrt{\frac{G}{\rho}}; \quad n = 1, 2, 3, \ldots; \text{ for torsional oscillations} \tag{4}$$

where $\omega_{n\mathrm{A}}$ and $\omega_{n\mathrm{T}}$ are nth circular (rad/s) natural frequencies for the axial and the torsional oscillations, respectively, n is the order of the mode, E, G, ρ and l_e equal, respectively, the axial Young's modulus, the shear modulus in the $z\theta$-plane, the mass density and the length of the cylindrical rod or tube. Eqs. (3) and (4) satisfy the relation

$$\nu = \frac{1}{2}\left(\frac{\omega_{n\mathrm{A}}}{\omega_{n\mathrm{T}}}\right)^2 - 1 \tag{5}$$

where ν is Poisson's ratio in the $z\theta$-plane. Here z-axis is along the axis of the cylindrical tube. We note that Eq. (5) involves frequencies of the axial and the torsional modes of vibration, and does not include any other material and geometric variable. Since Poisson's ratio of a linear elastic material is expected to be less than 0.5, therefore $\omega_{\mathrm{A}}/\omega_{\mathrm{T}}$ must be less than $\sqrt{3}$.

The frequency of RBM, in rad/s, of an infinitely long cylindrical thin tube of mean radius r_e and made of a linear elastic, homogeneous and transversely isotropic material with the axis of transverse isotropy along a radial line is given by [26]

$$\omega_{\mathrm{RBM}} = \frac{1}{r_e}\sqrt{\frac{E}{\rho(1-\nu^2)}} \tag{6}$$

For a tube of finite length Eq. (6) holds when the distance between axial nodes is much greater than the tube radius. Accordingly in Table 3, frequencies of RBMs derived from the present MD simulations are based on the distance between the axial nodes to be equal to the length of the tube, thus satisfying the condition for Eq. (6) to apply. Combining Eqs. (3), (4), and (6), we express the frequency of the RBM in terms of frequencies of the first axial and the first torsional modes as follows.

$$\omega_{\mathrm{RBM}} = \frac{2\omega_{\mathrm{T}} l_e}{\pi r_e}\left(4 - \left(\frac{\omega_{\mathrm{A}}}{\omega_{\mathrm{T}}}\right)^2\right)^{-1/2} \tag{7}$$

Besides frequencies of different modes of vibration, Eq. (7) involves the effective length and the effective radius of the continuum structure. We note that Eqs. (3), (4) and (6) are based on the assumptions that only one deformation mode is dominant. Accordingly, Young's moduli in the axial and circumferential directions appear, respectively, in Eqs. (3) and (6). The shear modulus and Poisson's ratio in the θz-plane appear in Eqs. (4) and (6) respectively.

6. Geometric and material parameters of an equivalent continuum structure

As pointed out above, frequencies of the second and the third modes of vibration of axial and torsional deformations of a SWCNT computed from the MM3 potential equal twice and thrice of the corresponding frequency of its first mode of vibration which also holds for a continuous linear elastic and homogeneous cylindrical body. Thus a necessary condition for the existence of an ECS is satisfied. Furthermore, frequencies of axial, torsional and RBM of vibration of a SWCNT computed from the MM simulations satisfy Eq. (7) in which ω_{RBM} is for a thin cylindrical tube. It is thus reasonable to assume that an ECS is a cylindrical tube, and its length equals that of the relaxed SWCNT. Then for the aspect ratio of the ECS to be equal to that of the SWCNT, it is necessary that the mean radius of the ECS tube be equal to that of the relaxed SWCNT. An ECS for a SWCNT is schematically shown in Fig. 3.

We now postulate that the thickness, Young's modulus and the shear modulus of the ECS are such that its frequency of free vibrations equals that of the corresponding SWCNT in all three modes of vibration. From frequencies computed using MD simulations, Poisson's ratio for the material of the ECS is determined by using Eq. (5) without assuming values for the thickness h, Young's modulus E and the shear modulus G. Values of Poisson's ratio of the ECS found from Eq. (5) are listed in Table 2. We note that Poisson's ratio of an ECS varies with its radius, depends upon the helicity of a SWCNT, and ν for an ECS of a

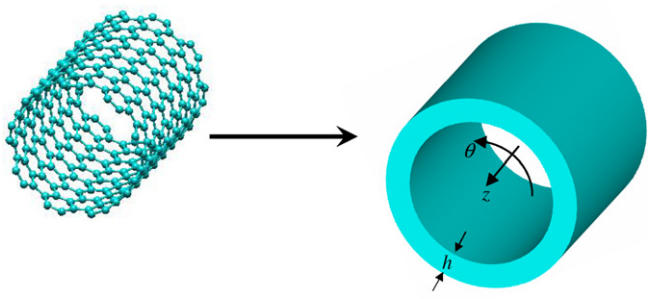

Fig. 3. Cylindrical tube equivalent in mechanical response to a SWCNT.

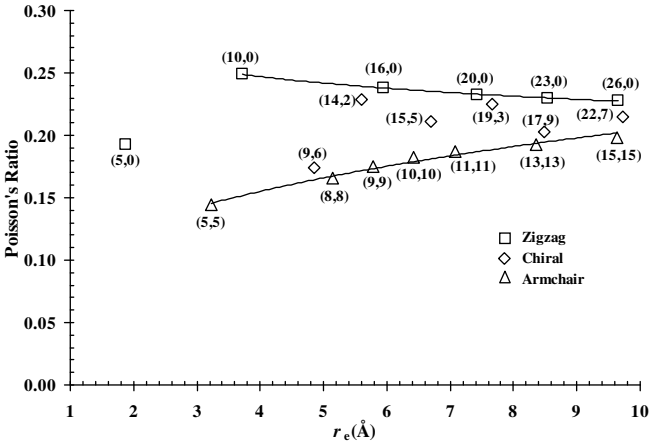

Fig. 4. Variation of Poisson's ratio of ECSs with the radius in the relaxed configuration of the corresponding SWCNTs.

zigzag SWCNT is usually higher than that for an ECS of an armchair SWCNT of the same diameter. The Poisson ratio of the ECS versus its mean radius is plotted in Fig. 4. For ECSs corresponding to zigzag and armchair SWCNTs, ν appears to converge to 0.23 and 0.20, respectively, while for chiral tubes it converges to 0.21. A similar trend has been reported in the literature for Poisson's ratios computed from *ab initio* calculations [6]. One reason for results for the (5,0) zigzag SWCNT not following the curve passing through data for other zigzag SWCNTs is that its radius is slightly larger than the bond length, and van der Walls forces may be playing a more significant role than that in tubes of larger radius. If so, results for the axial and the RBMs of vibrations of the ECS are not valid for this tube since these vibrations may change the distance between non-bonded atoms. With an increase in the radius of the SWCNT, the approximation improves and results for SWCNTs of diameters exceeding 6.4 Å lie on a smooth curve.

In Eqs. (3), (4), and (6), the thickness, h, of the EC cylindrical tube appears only through the mass density ρ. We assume that the thickness h equals 3.4 Å, and the mass of an ECS equals that of the SWCNT, i.e., the mass of all atoms in the SWCNT. Thus

$$\rho = \frac{m_c n_c}{\pi[(r_e + h/2)^2 - (r_e - h/2)^2] l_e} \tag{8}$$

where n_c and m_c, respectively, equal the number and the mass of carbon atoms in a SWCNT. With $m_c = 1.992(10)^{-26}$ kg, for each one of the SWCNTs studied, the average mass density ρ of the ECS is found to be 2491 kg/m^3. We can now use either Eq. (3) to find E or Eq. (4) to find G from the corresponding frequency computed using MD simulations; results are reported in Table 2. Average values of E, G and ν are also listed in the last row of Table 1. It is clear that presently computed values of E, G and ν match well with those obtained by other investigators who took $h = 3.4$ Å.

The values of E and G for the ECSs are nearly independent of the helicity and the diameter of their corresponding SWCNTs, and they satisfy the relation $E = 2G(1 + \nu)$. Thus we conclude that SWCNTs have axial Young's modulus $= 0.964 \pm 0.035$ TPa and shear modulus in the $z\theta$-plane $= 0.403 \pm 0.025$ TPa. Presently computed values of E are compared in Table 1 with those obtained by other investigators. It can be seen that the estimate of E based on the frequency of axial vibrations is in reasonable agreement with that obtained by most other investigators who used different techniques. Furthermore, values of the shear modulus listed in Table 2 are close to those found by using MD, structural mechanics, finite element, and MM simulations. The factor $(1 + \nu)$ in the relation $E = 2G(1 + \nu)$ reduces somewhat the dependence of G upon the SWCNT helicity and diameter. Recall that E is nearly a constant but ν varies with the SWCNT helicity and diameter.

Popov et al. [40] used a lattice dynamics model to study waves in an infinitely long SWCNT with force constants of the valence force field type which account for nearest-neighbor stretch, next-to-nearest-neighbor stretch, in-plane bend, out-of-plane bend and twist interactions. Their computed values of E increase with an increase in the tube radius, equaling about 0.857 GPa for tube radius of 2 Å and converge to 1 TPa for SWCNTs of radius exceeding 6 Å. For a given tube radius, E for an armchair tube is slightly less than that for a zigzag tube, and that for a chiral tube has an intermediate value. Presently computed values of E for armchair tubes are essentially independent of the tube radius. Recalling that the minimum radius of a tube considered here is 3.2 Å, our value of E agrees with that of Popov et al. [40]. For zigzag tubes studied herein, the radius varies from 1.87 Å to 9.64 Å. Whereas presently computed values of E are close to the converged value obtained by Popov et al. [40] they do not show the same trend when the tube radius is increased. For chiral tubes, presently computed values of E are virtually independent of the tube radius, equal the converged value computed by Popov et al. [40] and are both qualitatively and quantitatively consistent with their results since the minimum tube radius considered here is 4.86 Å. With an increase in the tube radius, the qualitative behavior of presently computed Poisson's ratio is opposite to that obtained by Popov et al. [40] even though the two sets of values are very close to each other. In each case, the converged value of Poisson's ratio equals about 0.2. Differences between our results and those of Popov et al. [40] can be attributed to different inter-atomic interaction effects in the two formulations, our not using a cut-off length and considering tubes of finite length. For example, the MM3 potential considers van der Walls forces and interactions between bond stretching and bending, and between bond stretching and twisting deformations.

7. Validation of the equivalent continuum structure

Sears and Batra [4] used MM3 potential to simulate static axial and torsional deformations of (16,0) SWCNT by applying essential boundary conditions (i.e. prescribing displacements of atoms) at the end faces. By computing the change in the diameter of a SWCNT during its axial deformations, they found Poisson's ratio by dividing the negative of the lateral strain by the axial strain. Poisson's ratio varied with the axial strain ε. They also postulated that for infinitesimal deformations of a SWCNT, its ECS is a linear elastic cylindrical tube of mean radius equal to the radius of the relaxed SWCNT. Their computations gave

$$E = \frac{1.18(10)^{-6}}{2\pi r_e h}\ Pa \tag{9}$$

$$G = \frac{1.72(10)^{-25}}{2\pi r_e h(r_e^2 + 0.25h^2)}\ Pa \tag{10}$$

Eq. (9) is obtained by setting $\varepsilon = 0$ in Eq. (2) of Ref. [4], and Eq. (10) is the same as Eq. (4) in Ref. [4]. Setting

$r_e = 5.935$ Å and $h = 3.4$ Å in Eqs. (9) and (10), we get $E = 0.93$ TPa, and $G = 0.356$ TPa which are close to the values obtained herein. Thus the ECS of a $(16,0)$ SWCNT is the same for static and free vibration problems.

We note that the frequency ω_{RBM} of a RBM given by Eq. (6) has not been used to ascertain E, G, ρ and h of the ECS. Thus, this relation can be employed to further validate the ECS. Frequencies of RBMs determined from Eq. (6) are listed in column 3 of Table 3. It is clear that they agree very well with those computed from the MD simulations.

8. Conclusions

We have used the MM3 potential to study free vibrations of the relaxed configuration of a single-walled carbon nanotube (SWCNT), and postulated that a continuum structure equivalent (ECS) to a SWCNT is a cylindrical tube of length and mean radius equal to those of the relaxed SWCNT, thickness 3.4 Å, and mass equal to that of all atoms in the SWCNT. The ECS is comprised of a linear elastic, homogeneous and transversely isotropic material with the axis of transverse isotropy coincident with a radial line of the SWCNT. Values of Poisson's ratio of the ECS are found from frequencies of axial and torsional vibrations and are independent of the wall thickness of the ECS. The mass density is found by requiring that the mass of the ECS equal that of all atoms in the SWCNT. Young's modulus and the shear modulus of the ECS are found by equating frequencies of axial and torsional modes of vibration of the ECS to those of SWCNT computed through numerical simulations using the MM3 potential. It is found that for various SWCNTs, Young's modulus equals 0.964 ± 0.035 TPa and the shear modulus in the $z\theta$-plane 0.403 ± 0.025 TPa. Poisson's ratio of the ECS depends upon the radius and the helicity of the underlying SWCNT, and converges to 0.23, 0.20 and 0.21 for zigzag, armchair and chiral SWCNTs respectively. Frequencies of radial breathing modes of vibration computed from the MM3 potential equal those of the ECS thereby validating material parameters for it. Also, presently computed values of Young's modulus and of the shear modulus of the ECS agree well with those obtained by using results of static simple tensile and torsional deformations.

Acknowledgements

This work was supported by the Office of Naval Research Grant N00014-98-06-0567 with Dr. Y.D.S. Rajapakse as the program manager. Views expressed in the paper are those of authors, and neither of the funding agency nor of their institutions.

References

[1] S. Iijima, Nature 354 (1991) 56–58.
[2] R.C. Batra, A. Sears, Int. J. Solid Struct. 44 (2007) 7577–7596.
[3] R.C. Batra, A. Sears, Modell. Simul. Mater. Sci. Eng. 15 (2007) 835–844.
[4] A. Sears, R.C. Batra, Phys. Rev. B 69 (2004) 235406.
[5] B.I. Yakobson, C.J. Brabec, J. Bernholc, Phys. Rev. Lett. 76 (1996) 2511–2514.
[6] D. Sanchez-Portal, E. Artacho, M.J.M. Soler, Phys. Rev. B 59 (1999) 12678.
[7] C. Goze, L. Vaccarini, L. Henard, P. Bernier, E. Hernandez, A. Rubio, Synth. Met. 103 (1999) 2500–2501.
[8] G. Zhou, W. Duan, B. Gu, Chem. Phys. Lett. 333 (2001) 344–349.
[9] S. Reich, C. Thomsen, P. Ordejon, Phys. Rev. B 65 (2002) 153407–153411.
[10] Y. Jin, F.G. Yuan, Compos. Sci. Technol. 63 (2003) 1507–1515.
[11] C. Li, T.W. Chou, Int. J. Solid Struct. 40 (2003) 2487–2499.
[12] T. Natsuki, K. Tantrakarn, M. Endo, Carbon 42 (2004) 39–45.
[13] H.W. Zhang, J.B. Wang, X. Guo, J. Mech. Phys. Solid 53 (2005) 1929–1950.
[14] X. Guo, J.B. Wang, H.W. Zhang, Int. J. Solid Struct. 43 (2006) 1276–1290.
[15] Y. Huang, J. Wu, K.C. Hwang, Phys. Rev. B 74 (2006) 245413.
[16] A.L. Kalamkarov, A.V. Georgiades, S.K. Rokkam, V.P. Veedu, M.N. Ghasemi-Nejhad, Int. J. Solid Struct. 43 (2006) 6832–6854.
[17] Y. Wu, X. Xhang, A.Y.T. Leung, W. Zhong, Thin Walled Struct. 44 (2006) 667–676.
[18] Y. Peng, L. Zhang, Q. Jin, B. Li, D. Ding, Physica E 33 (2006) 155–159.
[19] C.W.S. To, Finite Element. Anal. Des. 42 (2006) 404–413.
[20] K. Chandraseker, S. Mukherjee, Comput. Mater. Sci. 40 (2007) 147–158.
[21] P. Poncharal, Z.L. Wang, D. Urarte, W.A. de Heer, Science 283 (1999) 1513–1516.
[22] P.M. Agrawal, B.S. Sudalayandi, L.M. Raff, R. Komanduri, Comput. Mater. Sci. 38 (2006) 271–281.
[23] K. Sohlberg, B.G. Sumpter, R.E. Tuzun, D.W. Noid, Nanotechnology 9 (1998) 30–36.
[24] N. Yao, V. Lordi, J. Appl. Phys. 84 (1998) 1939–1943.
[25] A. Krishnan, E. Dujardin, T.W. Ebbesen, P.N. Yianilos, M.M.J. Treacy, Phys. Rev. B 58 (1998) 14013.
[26] C.Y. Wang, C.Q. Ru, A. Mioduchowski, J. Appl. Mech. 71 (2004) 622.
[27] N.L. Allinger, Y.H. Yuh, J. H Lii, J. Am. Chem. Soc. 111 (1998) 8551–8566.
[28] X. Zhou, J. Zhou, Z. Ou-Yang, Phys. Rev. B 62 (2000) 13692.
[29] J.W. Ponder, Computer Code Tinker Molecular Modelling Package 4.2, 2004.
[30] A.M. Rao, E. Richter, S. Bandow, B. Chase, P.C. Eklund, K.A. Williams, S. Fang, K.R. Subbaswamy, M. Menon, A. Thess, R.E. Smalley, G. Dresselhaus, M.S. Dresselhaus, Science 275 (1997) 187–191.
[31] E. Richter, K.R. Subbaswamy, Phys. Rev. Lett. 79 (1997) 2738.
[32] J. Kurti, G. Kresse, H. Kuzmany, Phys. Rev. B 58 (1998) 8869–8872.
[33] H. Kuzmany, B. Burger, M. Hulman, J. Kurti, A.G. Rinzler, R.E. Smalley, Europhys. Lett. 44 (1998) 518–524.
[34] R. Saito, T. Takeya, T. Kimura, G. Dresselhaus, M.S. Dresselhaus, Phys. Rev. B 57 (1998) 4145.
[35] H.M. Lawler, D. Areshkin, J.W. Mintmire, C.T. White, Phys. Rev. B 72 (2005) 233403–233406.
[36] V.N. Popov, P. Lambin, Phys. Rev. B 73 (2006) 85407.
[37] R.A. Jishi, L. Venkataraman, M.S. Dresselhaus, G. Dresselhaus, Chem. Phys. Lett. 209 (1993) 77–82.
[38] T. Chang, Acta Mech. Sini. 23 (2007) 159.
[39] R.D. Blevins, Formulas for Natural Frequencies and Mode Shapes, Van Nostrand Reinhold Company, New York, 1979.
[40] V.N. Popov, V.E. Van Doren, M. Balkanski, Phys. Rev. B 61 (2000) 3078.
[41] M.S. Dresselhaus, G. Dresselhaus, R. Saito, Carbon 33 (1995) 883.